Type III Secretion and Effectors Shape the Survival and Growth Pattern of *Pseudomonas syringae* on Leaf Surfaces[1][W][OA]

Jiyoung Lee[2], Gail M. Teitzel[2], Kathy Munkvold, Olga del Pozo[3], Gregory B. Martin, Richard W. Michelmore, and Jean T. Greenberg*

Department of Molecular Genetics and Cell Biology, University of Chicago, Chicago, Illinois 60637 (J.L., G.M.T., J.T.G.); Boyce Thompson Institute for Plant Research, Ithaca, New York 14853 (K.M., O.d.P., G.B.M.); Department of Plant Pathology and Plant-Microbe Biology, Cornell University, Ithaca, New York 14853 (G.B.M.); and The Genome Center, University of California, Davis, California 95616 (R.W.M.)

The bacterium *Pseudomonas syringae* pv *syringae* B728a (*Psy*B728a) uses a type III secretion system (T3SS) to inject effector proteins into plant cells, a process that modulates the susceptibility of different plants to infection. Analysis of *GREEN FLUORESCENT PROTEIN*-expressing *Psy*B728a after spray inoculation without additives under moderate relative humidity conditions permitted (1) a detailed analysis of this strain's survival and growth pattern on host (*Nicotiana benthamiana*) and nonhost (tomato [*Solanum lycopersicum*]) leaf surfaces, (2) an assessment of the role of plant defenses in affecting *Psy*B728a leaf surface (epiphytic) growth, and (3) the contribution of the T3SS and specific effectors to *Psy*B728a epiphytic survival and growth. On host leaf surfaces, *Psy*B728a cells initially persist without growing, and show an increased population only after 48 h, unless plants are pretreated with the defense-inducing chemical benzothiazole. During the persistence period, some *Psy*B728a cells induce a T3SS reporter, whereas a T3SS-deficient mutant shows reduced survival. By 72 h, rare invasion by *Psy*B728a to the mesophyll region of host leaves occurs, but endophytic and epiphytic bacterial growths are not correlated. The effectors HopZ3 and HopAA1 delay the onset of epiphytic growth of *Psy*B728a on *N. benthamiana*, whereas they promote epiphytic survival/growth on tomato. These effectors localize to distinct sites in plant cells and likely have different mechanisms of action. HopZ3 may enzymatically modify host targets, as it requires residues important for the catalytic activity of other proteins in its family of proteases. Thus, the T3SS, HopAA1, HopZ3, and plant defenses strongly influence epiphytic survival and/or growth of *Psy*B728a.

A major virulence component of the extracellular bacterial plant pathogen *Pseudomonas syringae* involves the injection of large repertoires of different effector proteins (often >25) into plant cells using a type III secretion system (T3SS; Greenberg and Vinatzer, 2003). Once inside plant cells, effectors can suppress host defenses, promote disease, and/or possibly elicit the release of nutrients (Chen et al., 2000; Lee et al., 2001; Nomura et al., 2005; Abramovitch et al., 2006; Chisholm et al., 2006; Rosebrock et al., 2007). Some plants can recognize individual effectors and activate defenses that result in the restriction of bacterial growth. Effector recognition is usually conditioned by a cognate plant resistance (R) protein(s), which when activated often induces localized programmed cell death, the accumulation of the signal molecule salicylic acid (SA), and global transcriptional reprogramming (Greenberg and Yao, 2004; Caplan et al., 2008; Lee et al., 2008). SA is important for basal resistance to *P. syringae* as well as some *R*-gene-mediated resistance responses (Delaney et al., 1994; Nawrath and Métraux, 1999; Feys et al., 2001; Rate and Greenberg, 2001). Exogenous application of SA or the synthetic agonist benzo (1,2,3) thiadiazole-7-carbothioic acid *S*-methyl ester (BTH) results in reduced pathogen growth (Uknes et al., 1992; Lawton et al., 1996).

Effectors that induce strong disease resistance were historically termed avirulence (Avr) effectors (Greenberg and Vinatzer, 2003). A number of characterized Avr effectors have large (qualitative) effects on pathogen fitness on specific hosts, causing large reductions in pathogen growth. However, recently it was found that *P. syringae* pv *syringae* strain B728a (*Psy*B728a) harbors

[1] This work was supported by the National Science Foundation (grant nos. DBI–0211823 and IOS–0822393 to R.W.M. and J.T.G. and DBI–0605059 to G.B.M.), the National Institutes of Health (grant no. R01 GM54292 to J.T.G.), a National Research Service Award (fellowship no. F32 GM754132 to G.M.T.), and the Korea Research Foundation Ministry of Education and Human Resources Development (fellowship no. KRF–200603520F00008 to J.L.).

[2] These authors contributed equally to the article.

[3] Present address: Instituto de Bioquímica Vegetal y Fotosíntesis, Consejo Superior de Investigaciones Científicas and Universidad de Sevilla, E–41092 Seville, Spain.

* Corresponding author; e-mail jgreenbe@midway.uchicago.edu.

The author responsible for distribution of materials integral to the findings presented in this article in accordance with the policy described in the Instructions for Authors (www.plantphysiol.org) is: Jean T. Greenberg (jgreenbe@midway.uchicago.edu).

[W] The online version of this article contains Web-only data.

[OA] Open Access articles can be viewed online without a subscription.

www.plantphysiol.org/cgi/doi/10.1104/pp.111.190686

several effectors that can quantitatively restrict pathogen growth on *Nicotiana benthamiana* even when disease ensues (Vinatzer et al., 2006). One possibility is that these effectors prevent the pathogen from causing too much host damage, and thus facilitate the cosurvival/coevolution of the pathogen and host.

Some *P. syringae* strains, such as *Psy*B728a, have a strong epiphytic phase (Wilson et al., 1999), in which the bacteria colonize leaf surfaces, called the phylloplane. Epiphytic bacteria must be able to withstand fluctuating wet and dry conditions, exposure to UV light, temperature fluctuations, and nutrient limitations. To protect themselves from these drastic conditions, one strategy is for bacteria to form aggregates. Surface-associated aggregates are often surrounded by exopolysaccharides that provide protection against desiccation, free radicals, and UV light and are important for epiphytic fitness (Yu et al., 1999; Wright et al., 2005; Chang et al., 2007). Bacteria also communicate with each other and other bacterial species on leaf surfaces through quorum sensing; this can also affect aggregate size (Dulla and Lindow, 2008). On snap bean (*Phaseolis vulgaris*) leaf surfaces, which *Psy*B728a colonizes very well, *Psy*B728a sometimes exists as some single cells, but a majority of the cells are found in aggregates of various sizes (Monier and Lindow, 2004). Many areas of leaf surfaces are not hospitable to bacteria, prompting the suggestion that access to nutrients is nonuniform in the phylloplane (Morris and Monier, 2003).

Another strategy for *P. syringae* to withstand fluctuating environmental conditions is to invade mesophyll regions and grow endophytically. Some strains of *P. syringae* produce coronatine, a metabolite mimic of Ile-conjugated jasmonic acid, which can facilitate bacterial entry into substomatal chambers (Melotto et al., 2006). *Psy*B728a does not produce coronatine, but instead makes syringolin A, which causes stomatal opening and counteracts stomatal innate immunity in snap bean and Arabidopsis (*Arabidopsis thaliana*; Schellenberg et al., 2010).

A majority of bacteria associated with leaves, including *P. syringae*, are on leaf surfaces (Wilson et al., 1999). Even before effectors were identified at the molecular level, epiphytic populations of *P. syringae* pv *syringae* on susceptible cultivars of snap bean were found to be larger than the populations on more resistant cultivars (Daub and Hagedorn, 1981). This is possibly due to the action of effectors. Field studies showed that T3SS-deficient *Psy*B728a does not survive well on snap bean and this reduced survival was hypothesized to be due to reduced epiphytic fitness (Hirano et al., 1999). Interestingly, *Psy*B728a lacking the effectors HopAA1 or HopZ3 have increased populations of bacteria that can be washed off *N. benthamiana* leaves several days after spray inoculation, a phenotype that can be reversed by adding back each gene on a plasmid (Vinatzer et al., 2006). *Psy*B728a lacking a functional T3SS also show a greatly reduced epiphytic population using this assay (Vinatzer et al., 2006). In contrast, endophytic HopAA1- or HopZ3-deficient *Psy*B728a grow similarly to the wild-type strain in the mesophyll region of the leaves (Vinatzer et al., 2006). This suggests a role for specific effectors in the epiphytic niche on some plants. An important caveat to this assertion is that leaf disc washes might be contaminated with endophytic bacteria.

In this study, we used quantitative microscopy to perform a detailed analysis of the roles of the T3SS, HopAA1, and HopZ3 in epiphytic fitness and the timing of the expression of effectors during *Psy*B728a associations with leaf surfaces kept under moderate relative humidity conditions. We show not only the importance of the T3SS in early epiphytic survival when effectors are beginning to be expressed, but also that HopAA1 and HopZ3 have host-specific roles in epiphytic fitness and localize to different subcellular sites in plant cells. We also show that activating the SA pathway results in the reduced population size of epiphytic bacteria. This suggests that effector interactions with epidermal cells and the signaling status of a major plant defense pathway play important roles in the early infection process.

RESULTS

The T3SS Is Necessary for Early Survival and Formation of Medium-Sized Bacterial Aggregates on Leaf Surfaces

Using leaf wash assays, T3SS-deficient (HrcC$^-$) *Psy*B728a show reduced epiphytic populations on spray-inoculated *N. benthamiana* (Vinatzer et al., 2006). In this assay, surface-associated bacteria harvested by gentle vortexing of leaf discs submerged in liquid are quantified by counting colony forming units (cfu). Endophytic bacteria might contaminate the epiphytic pool during this procedure. Therefore, we directly visualized GFP-labeled bacteria carrying *Ptrp-gfp* (gfp driven by a constitutive promoter) to assess the role of the T3SS in the epiphytic growth of *Psy*B728a on both *N. benthamiana* (a good host; Vinatzer et al., 2006) and tomato (*Solanum lycopersicum* 'Rio Grande-76R', a poor host; Lin and Martin, 2007). This approach permits the quantitative assessment of distributions of bacteria on leaf surfaces using epifluorescence microscopy (Monier and Lindow, 2003). Bacteria are quantified as fluorescence area per field imaged, analyzed using many random fields from multiple independent samples (see "Materials and Methods").

At 3, 24, and 48 h after spray inoculation of *N. benthamiana*, the average fluorescence area (5–7 μm^2, about three to six bacteria) of epiphytic *Psy*B728a did not significantly change (Fig. 1A). (Three hours was the earliest time at which the leaves were dry enough to accurately perform the assay.) At these early times, *Psy*B728a were found in similar distributions as isolated individual cells and in small groups, the majority of which (>95%) were less than 25 μm^2.

Between 48 and 72 h, there was a significant increase in the population size of *Psy*B728a ($P = 0.031$, Mann-Whitney test, $n = 47$; Fig. 1A).

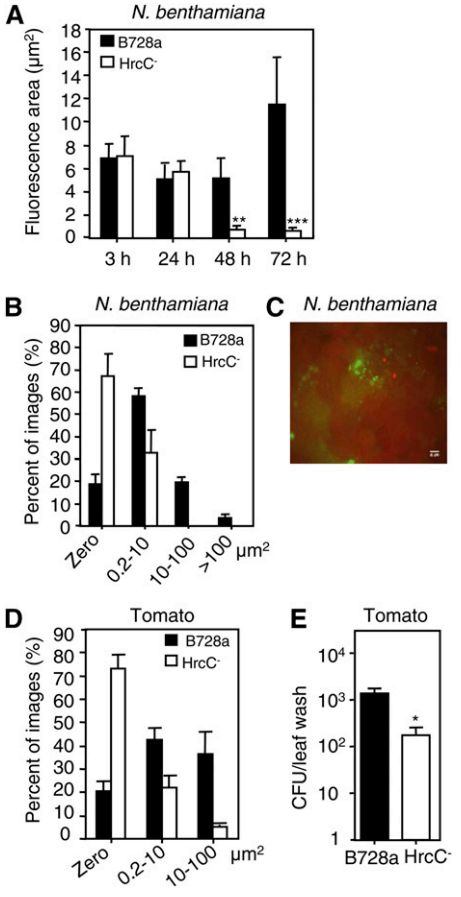

Figure 1. The T3SS is required for epiphytic growth of *Psy*B728a. *Psy*B728a and T3SS-deficient HrcC insertion mutant (HrcC⁻) were sprayed onto 17- to 21-d-old *N. benthamiana* and tomato 76R at an OD_{600} of 0.01. These experiments were repeated four or more times with similar results. All bars indicate SES. A, B, and D, Fluorescence area (or percent of images with a given fluorescence area) as a measure of bacterial area of GFP-expressing strains carrying *Ptrp-gfp* on the leaf surfaces at various times after spray inoculation. Leaf disks were viewed using epifluorescence microscopy. A, Population sizes of *Psy*B728a and HrcC⁻ on *N. benthamiana*. The *Psy*B728a population size did not change between 3, 24, and 48 h ($P > 0.08$, Mann-Whitney test, $n = 47$). At 72 h, the *Psy*B728a population was significantly greater than at 48 h ($P = 0.031$, Mann-Whitney test, $n = 47$). At 3 and 24 h, there was no significant difference between *Psy*B728a and HrcC⁻ ($P > 0.12$, Mann-Whitney test, $n = 46$–47). At 48 and 72 h, the HrcC⁻ epiphytic population was significantly reduced relative to *Psy*B728a at those times (**$P = 0.0074$, ***$P < 0.0001$, Mann-Whitney test, $n = 47$). B, The number of micrographs from 72 h populations that fell into different total fluorescence area categories was counted and the percentage from two independent experiments of the total images was determined. The categories were: zero (no bacteria present), 0.2 to 10 μm^2 (a few bacteria present), 10 to 100 μm^2 (a small aggregate), and >100 μm^2 (a medium aggregate). *Psy*B728a had significantly more micrographs that had larger amounts of bacteria and aggregates than HrcC⁻ ($P < 0.0001$, χ^2 test, $n = 48$). Using the Fisher's exact test with two categories: <10 μm^2 or >10 μm^2, also indicated that there were significantly more wild-type bacteria ($P < 0.0001$). C, Aggregates of *Psy*B728a/*Ptrp-gfp* that fluoresced green on *N. benthamiana* were primarily alive. A representative epifluorescence micrograph of *Psy*B728a/*Ptrp-gfp* on *N. benthamiana* 4 d after infection counterstained with propidium iodide, which preferentially stains dead cells with damaged membranes. A total of 252× magnification, scale bar is 20 μm. Green fluorescence marks all GFP-fluorescing bacteria. Red fluorescence marks dead, propidium-iodide-stained bacteria. Section shows green and red fluorescence merged images. D, Fluorescence area of GFP-expressing bacteria on the surface of tomato 76R leaves after 72 h. *Psy*B728a had significantly more micrographs that had larger amounts of bacteria and aggregates than HrcC⁻ ($P < 0.0001$, χ^2 test, $n = 48$). E, HrcC⁻ had a significantly lower bacterial population than *Psy*B728a as assayed using leaf washes after 72 h on tomato 76R (*$P < 0.05$, Mann-Whitney test, $n = 12$).

The average 3 and 24 h population sizes of HrcC⁻ and *Psy*B728a were similar. However, at 48 and 72 h the average fluorescence area of HrcC⁻ was greatly reduced relative to *Psy*B728a (Fig. 1A). This indicates a failure of the HrcC⁻ strain to survive well on leaf surfaces after 24 h. Furthermore, the distributions of bacteria per image were significantly different for *Psy*B728a and HrcC⁻ (Fig. 1B). At 72 h, the majority of the HrcC⁻ images either contained no or few bacteria, ranging from one to eight (0.2–10 μm^2). In contrast, for *Psy*B728a there were more images that contained a few bacteria (<10 μm^2). Importantly, there were also *Psy*B728a images with small (10–100 μm^2) and medium aggregates (>100 μm^2) that were not present at all following inoculation with the HrcC⁻ strain. In contrast, *Psy*B728a and HrcC⁻ grew similarly in culture and formed colonies of similar sizes and at similar rates on agar medium (data not shown).

To test if GFP-labeled *Psy*B728a were dead but fluoresced due to persistent GFP, bacteria on leaf discs were counterstained with propidium iodide. This dye does not penetrate intact membranes and therefore only stains dead bacteria. Red, dead bacteria were found in some instances. However, they were very few and the dead bacteria did not colocalize with green-fluorescing bacteria (Fig. 1C).

Unlike the medium-sized aggregates formed on *N. benthamiana* by 72 h, the epiphytic *Psy*B728a population on tomato lacked aggregates greater than 100 μm^2 (Fig. 1D). On tomato, HrcC⁻ also failed to survive well, occupying a significantly reduced fluorescence area of 2.4 ± 0.8 μm^2 relative to *Psy*B728a (7.9 ± 1.6 μm^2, $P < 0.0001$, Mann-Whitney test, $n = 48$). *Psy*B728a and HrcC⁻ showed different distributions of aggregate sizes (Fig. 1D). Most images of HrcC⁻ inoculated leaves contained no bacteria (zero). For *Psy*B728a, most images contained a few bacteria (0.2–10 μm^2, 43%) and small aggregates (10–100 μm^2, 36%), respectively.

When epiphytic bacteria were quantified using the leaf wash assay, there were significantly fewer HrcC⁻ bacteria than *Psy*B728a on *N. benthamiana* (Vinatzer et al., 2006) and tomato (Fig. 1E). After washing with vortexing, the epiphytic populations on leaf discs were greatly reduced as compared to before washing, as determined by epifluorescence microscopy indicating successful assessment of bacterial populations. A few bacteria (0.2–10 μm^2) remained on the leaf discs, but all aggregates greater than 10 μm^2 were removed.

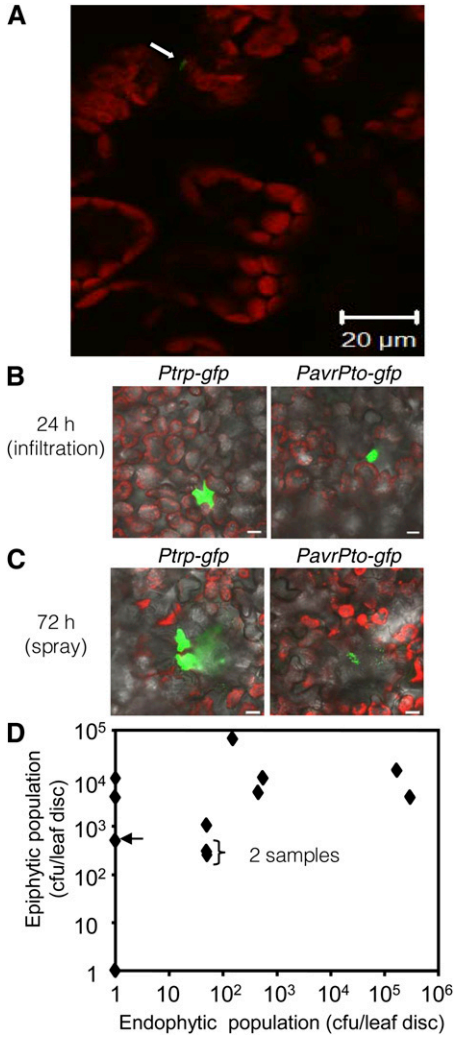

Figure 2. *Psy*B728a endophytic microcolonies are rarely detected after spray inoculation, and endophytic populations are not correlated with epiphytic populations. A, Single bacteria (white arrow) detected by confocal microscopy were detectable 3 h after low-dose infiltration (OD_{600} of 0.00001) into the intercellular mesophyll region. B and C, Microcolonies of GFP-labeled *Psy*B728a carrying *Ptrp-gfp* or *PavrPto-gfp* 24 h after infiltration directly into the mesophyll region were common, whereas 72 h after spray inoculation (as in Fig. 1) microcolonies were rare (see text). A to C, 400× magnification. Scale bar is 20 μm. D. Epiphtyic bacteria were quantified in leaf washes and endophytic bacteria were quantified after macerating washed and surface-sterilized leaf discs 72 h after spray inoculation. Bacteria were quantified from 12 leaf discs from independent plants. Each diamond represents epiphytic and endophytic bacteria enumerated from the same leaf disc. Some endophytic samples contained no bacteria, but are plotted as having a value of 1 due to the log scales of the axes. Arrow indicates the bacterial population at the start of the experiment. These experiments were repeated two or more times with similar results.

These results show (1) that conclusions drawn from the quantitative microscopy analysis and leaf wash assays are similar results, and (2) that possible endophytic bacterial contamination from the mesophyll region does not significantly affect conclusions about strain-to-strain differences in epiphytic populations using the wash assay. Furthermore, the microscopy analysis shows that the T3SS is important for survival prior to when bacteria populations increase on host leaf surfaces and probably also for survival on nonhost leaf surfaces when there is very limited bacteria growth or disease, as was the case on tomato.

Epiphytic Growth of *Psy*B728a on *N. benthamiana* Is Not Correlated with Endophytic Growth after Spray Inoculation

After spray inoculation, increased numbers of epiphytic *Psy*B728a may in part result from invasion to the intercellular mesophyll region followed by release of endophytic bacteria to leaf surfaces. To assess the degree to which bacteria originating from endophytic microcolonies can contribute to epiphytic populations,

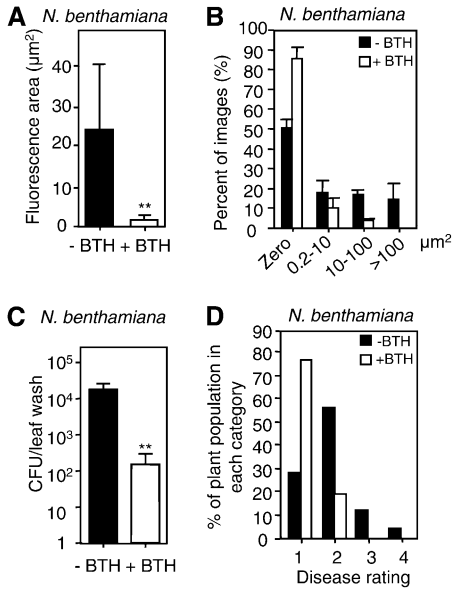

Figure 3. The epiphytic population of *Psy*B728a is reduced on BTH-treated *N. benthamiana*. Twenty-four hours after spraying 17- to 21-d-old *N. benthamiana* with 100 μM BTH, treated and control (untreated) plants were sprayed with *Psy*B728a at an OD_{600} of 0.01. These experiments were repeated three times with similar results. All bars indicate SES. A, Epiphytic bacterial area was significantly reduced on BTH-treated plants as measured by epifluorescence microscopy of *Psy*B728a/*Ptrp-gfp* on d 3 ($^{**}P < 0.005$, Mann-Whitney test, $n \geq 55$ or $^{*}P < 0.03$, unpaired t test using square-root-transformed data to account for differences in the data distribution). B, The number of micrographs from A that fell into the different indicated size categories were counted and the percentage of the total images was determined. There was a significant difference between BTH-treated and untreated plants using a χ^2 test ($P < 0.0001$, $n \geq 55$; Fisher's exact test, two categories: $<10\ \mu m^2$ or $>10\ \mu m^2$, $P < 0.0004$). C, Bacterial population of BTH-treated plants was significantly reduced as compared to untreated plants when measured using leaf washes (Mann-Whitney test, $^{**}P < 0.005$, $n = 10$). D, *Psy*B728a disease (small pin-prick spots) ratings were reduced on d 3 in BTH-treated plants as compared to untreated plants ($P < 0.0001$, Mann-Whitney test, $n = 25$–31). Ratings, expressed as percent diseased leaves/plant, were: 1, no disease; 2, ≤50%; 3, >50; and ≤75; 4, 100%.

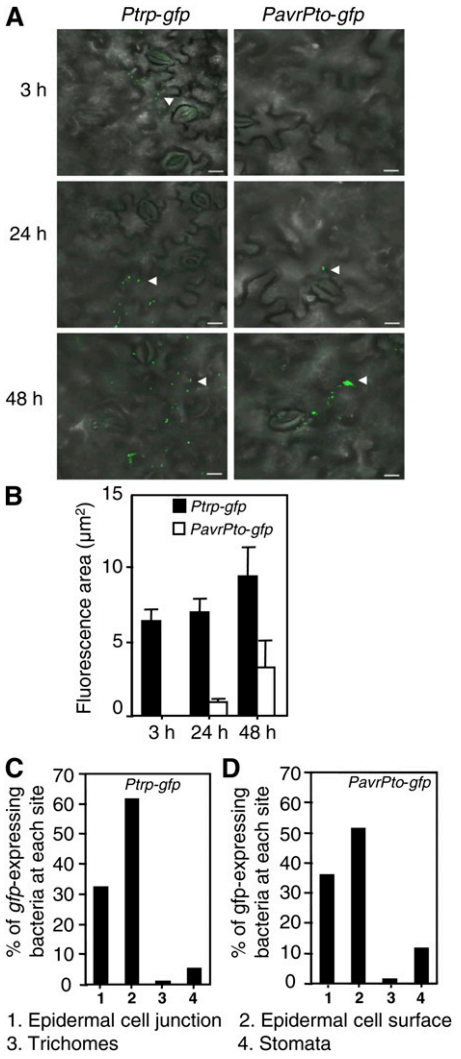

Figure 4. Type III effectors are expressed in leaf surface-associated bacteria. A, Timing of GFP expression in *Psy*B782a carrying *PavrPto-gfp* and *Ptrp-gfp*, respectively, inoculated on *N. benthamiana* leaf surfaces. White triangles indicate GFP-labeled bacteria. 400× magnification, scale bar is 20 μm. B, Data from A was quantified. White bars: fluorescence area of bacteria expressing GFP from *PavrPto-gfp*. Black bars: fluorescence area of bacteria expressing constitutive GFP from *Ptrp-gfp*. At least 48 pictures were analyzed for each strain. Bars indicate SES. There was no significant change in the fluorescence area of *Psy*B728a/*Ptrp-gfp* at the time points shown. The fluorescence area of *Psy*B728a/*PavrPto-gfp* was initially undetectable, but increased over time. These experiments were repeated three or more times with similar results. C and D, Cell types with which bacteria expressing GFP from *Ptrp-gfp* (C) and *PavrPto-gfp* (D) were associated on leaf surfaces. Bars indicate the percentage of GFP-expressing bacteria observed that were associated with epidermal cell junctions, epidermal cell surfaces, trichomes, and stomata of *N. benthamiana* at 24 h following inoculation of *Psy*B728a carrying *PavrPto-gfp* and *Ptrp-gfp*.

we characterized: (1) the propensity for bacteria to be released from newly formed endophytic microcolonies to leaf surfaces, (2) the frequency of endophytic microcolony formation after spray inoculation, and (3) whether the number of endophytic bacteria is correlated with epiphytic population size.

We used confocal microscopy to completely scan leaf discs for endophytic GFP-labeled *Psy*B728a after inoculation (approximately 1,791 fields/leaf disc). In two experiments, 3 h after very-low-dose infiltration (OD_{600} of 0.00001) into the intercellular mesophyll region, individual endophytic GFP-labeled *Psy*B728a/*Ptrp-gfp* bacterium were detected (Fig. 2A). By 24 h, we observed up to 130 fields among eight leaf discs with 1,635 ± 129 μm^2 (mean ± SE) endophytic microcolony fluorescence area/field with bacteria (Fig. 2B) in substomatal chamber (31.8%) and mesophyll cell regions (68.2%). Leaves were surface sterilized at the time of infiltration to allow monitoring of bacterial release to leaf surfaces. After 24 h, at sites where we found epiphytic bacteria, their population size averaged 44 bacteria on the leaf surface; most sites were associated with a microcolony under the epidermal layer (Supplemental Fig. S1). Most such microcolonies (83.3%) were associated with substomatal chambers, but some were mesophyll associated (9%). Thus, within 24 h a single bacterium in the mesophyll region can become a microcolony, which in some cases can release a small number of bacteria to the leaf surface (Fig. 2B). Later (after 48 h), lesions were visible on the leaves, at which time endophytic microcolonies were enlarged to 9,077 ± 331 μm^2 (n = 313) fluorescence area.

In three experiments, we also analyzed endophytic *Psy*B728a colonization after spray inoculation using confocal microscopy in which the entirety of eight discs per experiment was examined. Three and 24 h after spray inoculation, there were no GFP-labeled *Psy*B728a/*Ptrp-gfp* endophytic bacteria detected in any trials. By 48 h, among the three experiments, we observed a total of 0, 1, or 2 fields per eight leaf discs, with GFP-labeled endophytic *Psy*B728a clusters that showed 127.8 ± 16.8 μm^2 fluorescence area/field containing bacteria. By 72 h, endophytic microcolonies were present but rare: Each leaf disc had one or no fields containing GFP-labeled *Psy*B728a microcolonies at 1,791 ± 649 μm^2 fluorescence area/field containing *Psy*B728a (Fig. 2C). The timing of appearance and the size of most endophytic microcolonies indicates that most were only newly formed by 72 h after spray inoculation, similar to 24 h microcolonies after infiltration. If these microcolonies behave similar to those observed 24 h after infiltration, each leaf disc would have <50 bacteria that were released from the endophytic pool to the leaf surfaces, or a small fraction of the total epiphytic pool, at 72 h after spray inoculation.

At 72 h, we also enumerated epiphytic bacteria after leaf washes and subsequently quantitated endophytic bacteria in the same leaf discs. Some leaf discs had similar epiphytic populations (7×10^3–2×10^4 cfu), but had widely differing endophytic populations (from 0–5×10^5 cfu; Fig. 2D). In this experiment, some endophytic bacteria may be lost during the leaf washes, but this should occur similarly between leaf discs and would not account for the wide differences

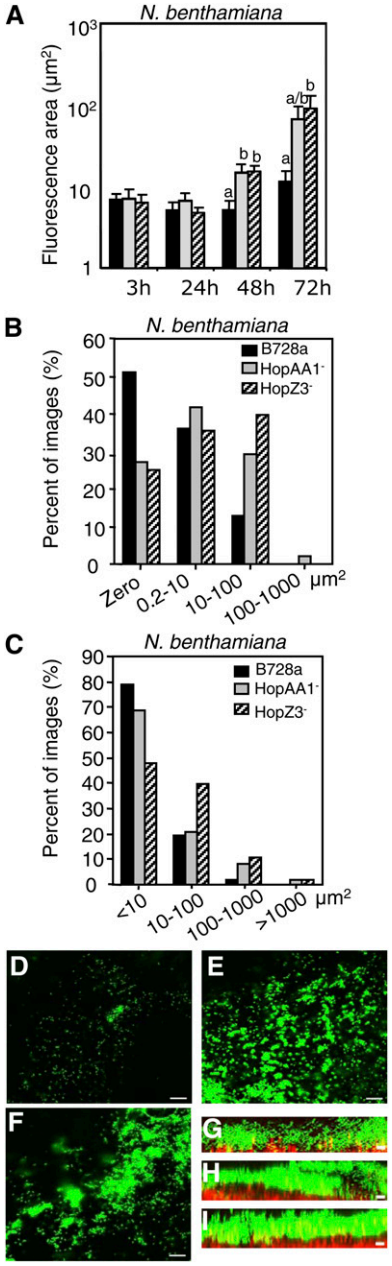

Figure 5. HopAA1 and HopZ3 restrict the epiphytic population of *Psy*B728a on *N. benthamiana*. A to C, Quantitation of bacteria viewed on leaf surfaces by epifluorescence microscopy after spray inoculation. These experiments were repeated three or more times with similar results. Bars indicate SES. Green fluorescence area expressed from *Ptrp-gfp* was quantified as a measure of the amount of bacteria associated with the surface. A, Early population sizes (3, 24 h) of *Psy*B728a, HopAA1⁻, and HopZ3⁻ were similar ($P > 0.13$, Mann-Whitney test, $n = 47$). At 48 h, HopAA1⁻ and HopZ3⁻ populations were increased compared to *Psy*B728a (at each time point, each letter group differs from other letter groups at a level of $P < 0.004$ or less, Mann-Whitney test, $n = 47$). Fisher's exact test using two categories: <10 μm^2 or >10 μm^2, also showed significant differences: $P < 0.0039$ (*Psy*B728a and HopAA1⁻), $P < 0.0001$ (*Psy*B728a and HopZ3⁻). This experiment was done together with HrcC⁻ bacteria (see Fig. 1A). Thus, the *Psy*B728a data are the same as that shown in Figure 1A. B and C, At 48 h (B) and 72 h (C) HopZ3⁻ and HopAA1⁻ had a greater amount of larger aggregates than *Psy*B728a. χ^2 tests of the distributions at the two time points were each significantly different between the deletion mutants and *Psy*B728a ($P < 0.0001$, $n = 47$). D to I, Five days after spray inoculations, HopZ3⁻ and HopAA1⁻ had larger and thicker aggregates than *Psy*B728a on *N. benthamiana*. Confocal projections of aggregates near disease lesions of GFP-expressing (from *Ptrp-gfp*) *Psy*B728a (D), HopAA1⁻ (E), and HopZ3⁻ (F) from d 5 with a magnification of 400×. Scale bar is 20 μm. Cross-section views of the thicknesses of bacterial aggregates on leaf surfaces of *Psy*B728a (G), HopAA1⁻ (H), and HopZ3⁻ (I). Sagittal images were created from a collection of 26 to 91 images at a 0.5-μm interval. Autofluorescence of chlorophyll is depicted in red. Scale bar is 10 μm.

in endophytic populations that we observed. Additionally, epiphytic *Psy*B728a attained a population of nearly 10^5 cfu on one leaf disc that yielded only 200 cfu from the intercellular mesophyll region (Fig. 2D). Thus, after spray inoculation, there was no correlation between epiphytic and endophytic populations; endophytic bacteria were too few in most samples to account for the significant increases in epiphytic populations at 72 h.

Activation of the SA Defense Pathway Restricts Epiphytic Growth

To test whether known plant defenses affect epiphytic bacterial populations, the SA agonist BTH was sprayed onto *N. benthamiana* 24 h prior to spray inoculation with *Psy*B728a. Three days after infection, the fluorescence area of epiphytic *Psy*B728a/*Ptrp-gfp* on BTH-treated leaves was much smaller than the area found on untreated leaves (Fig. 3A). The distributions of aggregates between BTH-treated and -untreated leaves were different, with images from BTH-treated leaves lacking medium aggregates of >100 μm^2 (Fig. 3B). In addition, the bacterial population recovered using the wash assay was also significantly reduced in BTH-treated leaves as compared to untreated leaves (Fig. 3C). Spray inoculation resulted in disease symptoms of small, discolored patches on *N. benthamiana* leaves. As expected, BTH pretreatment suppressed these disease symptoms. On d 3, the percentage of inoculated leaves with symptoms was significantly reduced in BTH-treated plants (Fig. 3D). BTH is thought not to possess antimicrobial activity, but rather acts indirectly as a defense-inducing SA agonist (Friedrich et al., 1996). Therefore, these results suggest that SA-induced defenses can limit epiphytic bacterial growth and reduce the incidence of disease.

P. syringae B728a Expresses Type III Effectors on the Leaf Surface

The early reduced fitness of HrcC⁻ bacteria on leaf surfaces indicated the possibility that *P. syringae* uses the T3SS on the leaf surface. Since a direct in vivo secretion assay for surface-associated bacteria is not yet available, we used expression of a T3SS reporter as a proxy for possible secretion. Specifically, we intro-

Table I. *Quantitative analysis of biofilm-like structures on N. benthamiana on d 5*

Strain	Microcolony Surface Area[a,b]	Thickness[b,c]
	μm^2	μm
*Psy*B728a	308.3 ± 106.8	15.7 ± 1.7
HopAA1$^-$	1,763.8 ± 328.8 ($P < 0.0001$)	22.5 ± 2.3 ($P = 0.025$)
HopZ3$^-$	1,695.8 ± 337.1 ($P < 0.0001$)	21.7 ± 2.3 ($P = 0.18$)

[a]Microcolony surface area per view. Values are means ± SES of the means ($n = 38$). [b]Mann-Whitney test was performed for statistical analysis. [c]Height from the epidermal cell surface to the top of bacterial aggregates. Values are means ± SES of the means ($n = 7$–10). Cross-section images (z stack) were created from a collection of 26 to 91 plane images (*x*-*y*) at 0.5-μm intervals. Vertical cross-section (*x*-*z*) images were generated with a laser scanning microscope image browser.

duced a previously characterized reporter, an effector promoter fused to GFP (*PavrPto-gfp*; Xiao et al., 2004) into *Psy*B728a. If bacterial effectors are expressed during epiphytic growth, GFP should be visible.

After spray inoculation of *N. benthamiana*, bacterial populations that retained *gfp* plasmids were very similar in *Psy*B728a carrying *Ptrp-gfp* or *PavrPto-gfp*, as assayed using leaf washes (Supplemental Fig. S2); both strains elicited similar disease symptoms after 3 to 4 d. Three hours after spraying, no GFP-positive *Psy*B728a/*PavrPto-gfp* bacteria were visible (Fig. 4, A and B). However, by 24 and 48 h, some *Psy*B728a/*PavrPto-gfp* bacteria were positive for GFP on *N. benthamiana* leaf surfaces. *Psy*B728a/*Ptrp-gfp* bacteria were positive for GFP at all time points tested and showed similar fluorescence areas at 3, 24, and 48 h (Fig. 4B). Fewer *Psy*B728a/*PavrPto-gfp* bacteria were fluorescent compared with *Psy*B728a/*Ptrp-gfp.* Estimating the fluorescence area of *Psy*B728a/*Ptrp-gfp* to be 100% of the bacterial cells at a given time point, 12.9% of *Psy*B728a/*PavrPto-gfp* cells fluoresced after 24 h and 34.5% of *Psy*B728a/*PavrPto-gfp* cells fluoresced after 48 h (Fig. 4, A and B). Plant epidermal cells in contact with fluorescent *Psy*B728a/*PavrPto-gfp* did not appear to die or form microlesions up to 48 h. Cell death is usually associated with high autoflorescence under UV and cell shrinkage (Greenberg and Yao, 2004). However, epidermal cells in contact with fluorescent *Psy*B728a/*PavrPto-gfp* bacteria showed no change in their UV fluorescence and maintained their turgid appearance in differential interference contrast images (Supplemental Fig. S3; Fig. 4A).

Generally, the fluorescence area of the mesophyll-associated *Psy*B728a/*PavrPto-gfp* bacteria was smaller than that of *Psy*B728a/*Ptrp-gfp* (Fig. 2, B and C). Thus, effectors are expressed in a subpopulation of epiphytic bacteria before colonization of the mesophyll region, and only a subset of the total population may synthesize and secrete effectors during the bacterial associations with plant cells.

To determine whether effector expression occurred preferentially at particular sites of the leaf surface, we first quantified the relative distribution of the bacteria on *N. benthamiana* leaf surfaces 24 h after inoculation. Most *Psy*B728a/*Ptrp-gfp* bacteria were associated with the epidermal cell surface and cell junctions, although a small percentage of bacteria were associated with trichomes and stomata (Fig. 4C). Effector gene-expressing bacteria were observed in a similar pattern mainly at the epidermal cell surface and epidermal cell junctions (Fig. 4D; Supplemental Fig. S4). Thus, the sites of effector expression parallel the sites where most bacteria are present.

Effectors Influence the Survival and Size of the Epiphytic Populations on Leaves

Previous experiments using leaf washes after spray infection suggest that in *Psy*B728a, HopZ3 and HopAA1 may have roles in the epiphytic niche (Vinatzer et al., 2006). We sought to rule out that the leaf wash results with HopZ3$^-$ and HopAA1$^-$ *Psy*B728a were biased due to contaminating endophytic bacteria and to compare the roles of HopZ3 and HopAA1 on host and nonhost plants. Therefore, we further characterized the epiphytic behaviors of the HopZ3$^-$ and HopAA1$^-$ strains carrying *Ptrp-gfp* after spray inoculation using microscopy.

The HopAA1$^-$ or HopZ3$^-$ strains each showed a similar level of survival to *Psy*B728a that did not change between 3 and 24 h on *N. benthamiana*, as measured using epifluorescence microscopy (Fig. 5A). At 48 and 72 h, HopZ3$^-$ and HopAA1$^-$ showed significantly different population distributions that favored increased aggregate sizes, as compared to *Psy*B728a (Fig. 5, B and C). At 72 h, *Psy*B728a had no large aggregates (>1,000 μm^2), while these were present, albeit rarely, for HopZ3$^-$ and HopAA1$^-$ (Fig. 5C). Scanning confocal laser microscopy revealed that compared to *Psy*B728a aggregates on d 5, aggregates of HopZ3$^-$ and HopAA1$^-$ had more developed (Fig. 5, D–F; Table I) and/or thicker appearances (Fig. 5, G–I; Table I). Similar to the microscopy results, leaf washes confirmed increased growth of HopZ3$^-$ and HopAA1$^-$ relative to *Psy*B728a, which was not accompanied by increased endophytic populations of HopZ3$^-$ or HopAA1$^-$ at 48 h (Supplemental Fig. S5).

In contrast to the results with *N. benthamiana* inoculations, epiphytic populations of HopZ3$^-$ and HopAA1$^-$ carrying *Ptrp-gfp* on tomato 76R were reduced, similar to HrcC$^-$, compared with *Psy*B728a after 72 h. The majority of the HopZ3$^-$ and HopAA1$^-$ images

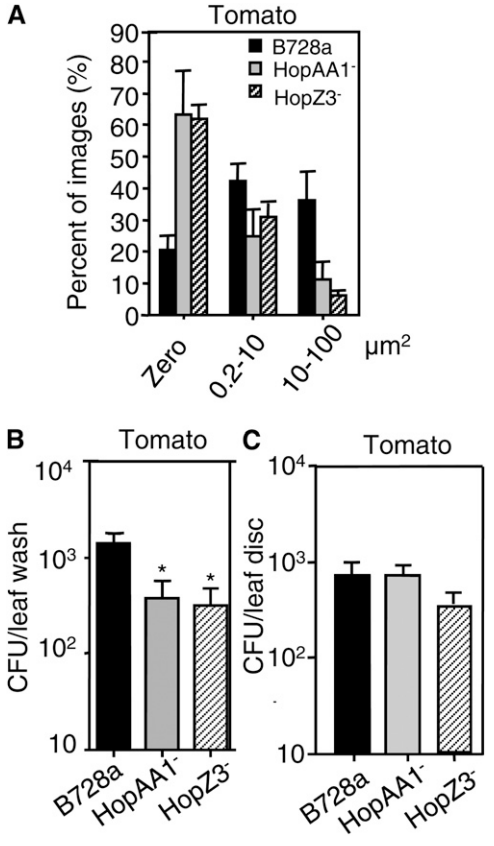

Figure 6. HopAA1 and HopZ3 are important for epiphytic fitness of *Psy*B728a on tomato 76R. *Psy*B728a and mutants carrying *Ptrp-gfp* at an OD_{600} of 0.01 were sprayed onto 17- to 21-d-old tomato 76R. All bars indicate SES. A, After 72 h, the populations of HopZ3$^-$ and HopAA1$^-$ were reduced compared to *Psy*B728a. A χ^2 test indicated that the distributions were significantly different between the deletion mutants and *Psy*B728a (HopAA1$^-$, $P < 0.0001$, $n \geq 48$; HopZ3$^-$, $P < 0.0001$, $n \geq 48$). This experiment was done together with HrcC$^-$ bacteria (see Fig. 1D). Thus, the *Psy*B728a data are the same as that shown in Figure 1D. B, Leaf disks were washed to remove and enumerate bacteria in the attached biomass. Reductions in the mutant bacterial populations compared with *Psy*B728a after 72 h were statistically significant (*$P < 0.05$, Mann-Whitney test, $n = 12$). C, Endophytic bacteria population of HopAA1$^-$ and HopZ3$^-$ from Figure 6B was not significantly different compared with *Psy*B728a after 72 h (HopAA1$^-$, $P = 0.90$, HopZ3$^-$, $P = 0.3556$, $n \geq 12$ for both). These experiments were repeated twice with similar results.

either contained no or few bacteria (<10 μm^2). In contrast, there were more images of *Psy*B728a that contained a few bacteria (<10 μm^2) or small bacterial clusters (10–100 μm^2; Fig. 6A). There were also significantly fewer surface-associated HopAA1$^-$ and HopZ3$^-$ bacteria than *Psy*B728a on tomato, as assayed using leaf washes (Fig. 6B). No significant differences were found in the levels of endophytic HopAA1$^-$ and HopZ3$^-$ versus *Psy*B728a (Fig. 6C; Vinatzer et al., 2006). Thus, whether HopAA1 and HopZ3 suppress or promote epiphytic bacterial growth and/or survival depend on the host genotype/species on which the bacteria reside.

HopZ3, HopAA1, or a T3SS Does Not Affect Bacterial Attachment to Surfaces

It seemed possible that epiphytic population size might be influenced if the T3SS or individual effectors affect bacterial attachment to surfaces. First, we checked the early population size at 3 and 24 h after bacteria had been sprayed onto leaves (Figs. 1A and 5A). There was no difference in the levels of HrcC$^-$, HopZ3$^-$, or HopAA1$^-$ relative to *Psy*B728a, indicating that the same number of bacteria initially adhered to *N. benthamiana*. The relative abilities of HopZ3$^-$, HopAA1$^-$, HrcC$^-$, and *Psy*B728a to attach to plastic and glass surface were also similar after culturing cells under conditions that promoted effector expression and secretion (He et al., 1993; Fig. 7, A and B). Thus, differences in attachment did not account for the strain-to-strain alterations in epiphytic population distributions that we observed.

HopZ3 or HopAA1 Do Not Affect the Release of Endophytic Bacteria onto Leaf Surfaces

Larger epiphytic communities might occur if effectors promote the release of mesophyll-associated endophytic bacteria onto leaf surfaces. Therefore, we examined the ability of endophytic *Psy*B728a/*Ptrp-gfp* and its derived strains to be released from the mesophyll region onto leaf surfaces. Bacteria were syringe inoculated into leaves that were subsequently surface sterilized and examined to ensure that there were no GFP-expressing epiphytic bacteria at the beginning of the experiment. After 48 h, more *Psy*B728a cells were released to the leaf surface from the intercellular region than HrcC$^-$. This may reflect the reduced fitness of endophytic HrcC$^-$ *Psy*B728a on *N. benthamiana* (Vinatzer et al., 2006). In contrast, there was no difference in the numbers of released *Psy*B728a, HopZ3$^-$, and HopAA1$^-$ or in their endophytic populations (Fig. 7, C–E; Supplemental Fig. S6; Vinatzer et al., 2006). Thus, increased epiphytic populations of HopZ3$^-$ and HopAA1$^-$ strains after spray inoculation is not due to enhanced endophytic growth or release to leaf surfaces.

HopZ3 and HopAA1 Localize to Different Sites within Plant Cells

To gain insight into where and how HopZ3 and HopAA1 might act within plant cells, C-terminal fusions of HopZ3 and HopAA1 to GFP were transiently expressed and localized in *N. benthamiana*. HopAA1-GFP fluorescence was visible at the cell periphery (Fig. 8A). Mature plant cells have a large vacuole and thin cytoplasm, making it difficult to distinguish cytoplasmic from plasma membrane or tonoplast membrane localization. However, HopAA1-GFP is likely at the plasma membrane, since the protein was only detected in the membrane fraction in *N. benthamiana* (Fig. 8B) and GFP was visible closer to the cell edges than chloroplasts, which are located in

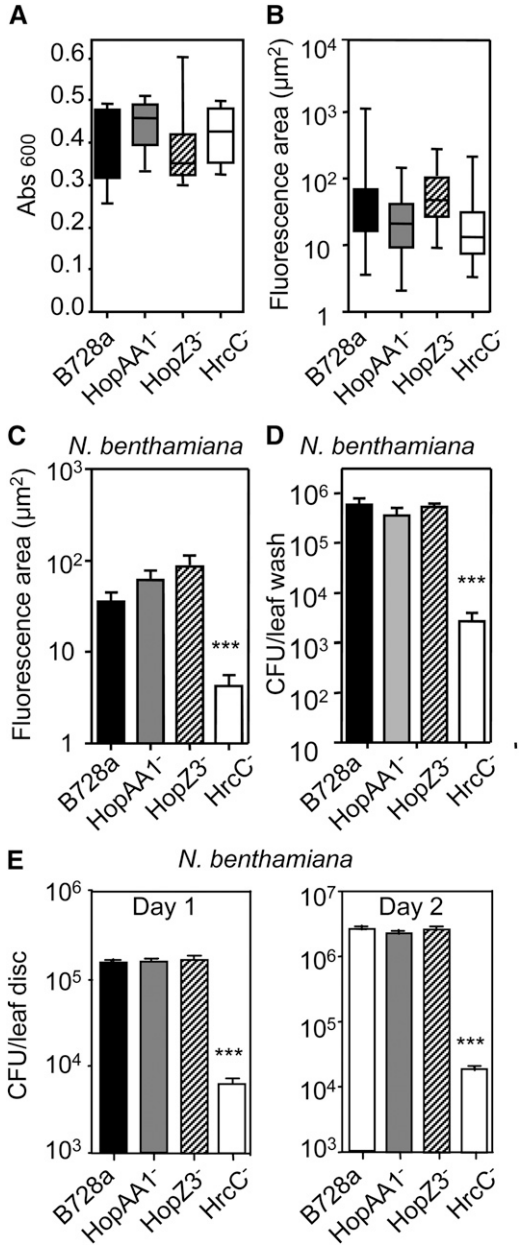

Figure 7. Effect of the loss of HopAA1, HopZ3, and HrcC on bacterial attachment to plastic and glass substrates and endophytic growth and bacterial release onto leaf surfaces. A, The ability of *Psy*B728a, HopAA1$^-$, HopZ3$^-$, and HrcC$^-$ to attach to a plastic microtiter plate was not different ($P > 0.19$, *t* test, $n = 8$). *Psy*B728a, HopAA1$^-$, HopZ3$^-$, and HrcC$^-$ were inoculated at an OD_{600} of 0.1 in effector-inducing minimal media in a microtiter plate. After 24 h, the supernatant was removed and the attached biomass stained with 1% crystal violet was measured after dissolving the dye in ethanol. Bars indicate SES. B, Attachment of GFP-expressing *Psy*B728a, HopAA1$^-$, HopZ3$^-$, and HrcC$^-$ carrying *Ptrp-gfp* onto glass coverslips over 3 h was not different ($P > 0.055$, *t* test, $n = 27–36$). The bacterial area per image was determined for at least 25 randomly taken images. C and D, Release of mesophyll-associated bacteria onto leaf surfaces after 48 h was similar between *Psy*B728a, HopAA1$^-$, and HopZ3$^-$, while HrcC$^-$ was reduced. Four-week-old *N. benthamiana* were injected with strains carrying *Ptrp-gfp* and surface sterilized to remove GFP-expressing bacteria. C, The fluorescence area of each strain released to the surface was quantified using epifluorescence microscopy. HopAA1$^-$ and HopZ3$^-$ populations were not significantly different from *Psy*B728a ($P > 0.66$, Mann-Whitney test, $n \geq 48$), while HrcC$^-$ had a significantly reduced epiphytic population (***$P < 0.0001$, Mann-Whitney test, $n \geq 48$). D, Bacterial populations of HopAA1$^-$ and HopZ3$^-$ were not significantly different from *Psy*B728a ($P > 0.16$, $n = 12$), while HrcC$^-$ had a significantly reduced epiphytic population, as assayed using leaf washes (***$P < 0.0001$, Mann-Whitney test, $n = 12$). E, Bacterial population of HopAA1$^-$ and HopZ3$^-$ when inoculated to the intercellular region were not significantly different from *Psy*B728a ($P > 0.38$), while HrcC$^-$ had a significantly reduced endophytic bacteria population on days 1 and 2 (***$P < 0.005$, $n = 8$). These experiments were repeated three or more times with similar results. Bars indicate SES.

the region between the tonoplast and plasma membrane (Supplemental Fig. S7). Bioinformatic analysis using two different structure prediction programs indicated that HopAA1 may contain between one and three transmembrane regions, possibly exposing a portion of the protein to the extracellular milieu.

HopZ3-GFP was localized to the nucleus and the cell periphery (Fig. 8, A and C). In this case, the cell periphery is probably the cytoplasm, since HopZ3 was previously only found to be in the soluble fraction when produced in *N. benthamiana* (Lewis et al., 2008). The GFP fluorescence was from the intact 75-kD fusion proteins, since there was no evidence of the GFP monomer in extracts, as determined by western-blot analysis (Fig. 8D). These results indicate that HopAA1 likely exerts its function at the membrane, whereas HopZ3 may act in the nucleus and/or cytoplasm.

Conserved Potential Catalytic Residues in HopZ3 Are Involved in Its Function

Since HopZ3 has similarity to the C55 family of Cys proteases (Lewis et al., 2008), we tested whether the potential catalytic residues C300, H243, and E263 were important for HopZ3's function. Several mutations did not affect the stability or localization of HopZ3-GFP in *N. benthamiana* or HopZ3-HA accumulation in *Psy*B728a (Figs. 8D and 9A; Supplemental Fig. S8). Therefore, we tested the HopZ3 variants in three assays in which HopZ3 showed a phenotype.

The HA-epitope-tagged HopZ3 variants H243L and H243A retained the ability to complement the HopZ3$^-$ mutation for suppression of epiphytic growth on *N. benthamiana.* However, the variants C300A, C300R, C300W, and E263A failed to complement the HopZ3$^-$ mutation (Fig. 9A). HopZ3 does not induce cell death, but interferes with AvrPto1-induced cell death when both effectors are transiently expressed in *N. benthamiana* (Vinatzer et al., 2006). When GFP fusions of HopZ3-GFP and its variants were coexpressed with AvrPto1-GFP (Fig. 9B), the E263A, C300A, C300R, C300W, H243L, and H243A variant proteins no longer abrogated cell death (Fig. 9C).

Fortuitously, we found that HopZ3 elicited mild cell death on transgenic *N. benthamiana* that ectopically

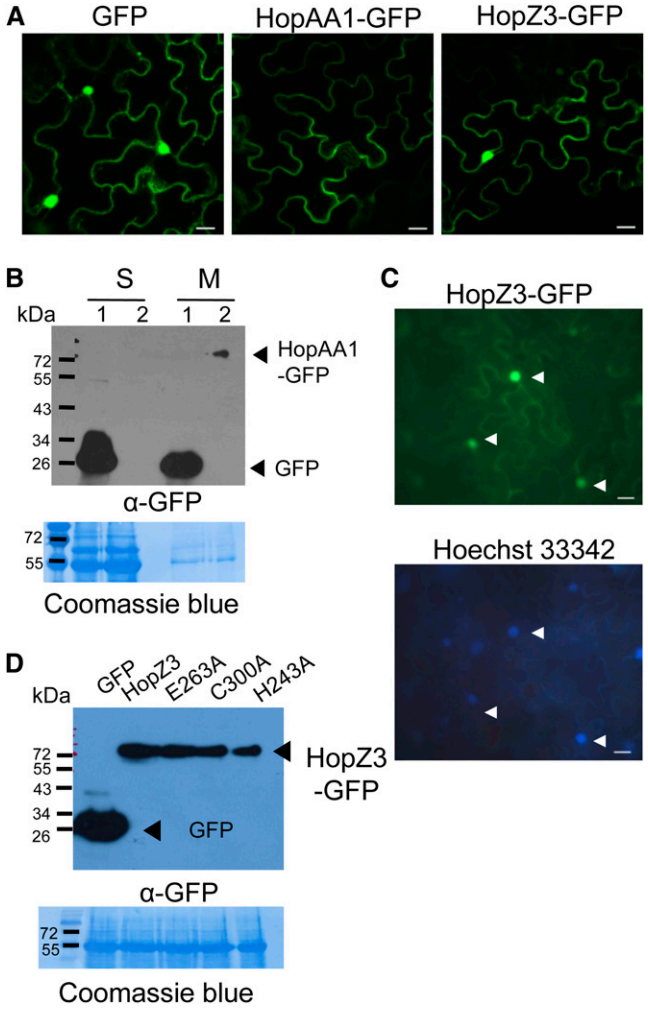

Figure 8. HopZ3-GFP and HopAA1-GFP show different subcellular localization in planta. *N. benthamiana* was transiently transformed with *A. tumefaciens* carrying *hopZ3-gfp* or *hopAA1-gfp*. A, GFP fluorescence detected using confocal microscopy. Left: GFP control showing fluorescence at the cell periphery and nucleus; middle: HopAA1-GFP detected predominantly at the cell periphery (probably the plasma membrane, see B); right: HopZ3-GFP detected at the cell periphery (probably the cytosol, see main text) and nucleus. 400× magnification, scale bar is 20 μm. B, Immunoblot analysis of soluble and membrane protein fractions from GFP- and HopAA1-GFP-expressing *N. benthamiana* leaves. 1: GFP, 2: HopAA1-GFP. HopAA1-GFP was only found in the membrane fraction. The bottom section shows a Coomassie-Blue-stained membrane as loading control. C, HopZ3-GFP fluorescence at the cell peripheries and nuclei as visualized by epifluorescence microscopy and counterstaining with Hoechst 33342 to mark nuclei. White triangles indicate nuclei. 400× magnifications, scale bar is 20 μm. D, Immunoblot of proteins extracted from *N. benthamiana* expressing GFP; GFP signal of HopZ3-GFP and HopZ3-GFP variants are not cleaved GFP products. Samples in B and D were run on a 10% polyacrylamide gel. The bottom section shows a Coomassie-Blue-stained membrane as loading control. These experiments were done three times with similar results.

expressed the tomato *R* gene *Pto* (Supplemental Fig. S9) or when HopZ3 and Pto were transiently coexpressed (Table II; Supplemental Table S1). This phenotype was unexpected, but not unique. AvrB3, an unrelated *Psy*B728a effector, but not several other effectors, also elicited *Pto*-dependent cell death (Supplemental Fig. S10). Elevated defense signaling due to Pto overexpression (as was documented in tomato; Tang et al., 1999) might explain why HopZ3 and AvrB3 elicited cell death in *N. benthamiana*/*Pto*. Alternatively, Pto might have a low-affinity interaction with HopZ3 and/or AvrB3 in planta that triggers cell death due to protein overexpression. However, we found no evidence for an interaction of Pto with HopZ3 or AvrB3 (Supplemental Fig. S11). All the HA-epitope-tagged HopZ3 point mutants were expressed (Fig. 9D) and all except H243A and H243L lost the ability to cause cell death on *N. benthamiana*/*Pto* (Fig. 9E). Data from the different assays suggests that the potential catalytic residues C300, E263, and H243 of HopZ3 are important for one or more phenotypes conferred by HopZ3.

DISCUSSION

*Psy*B728a associated with plant leaves exhibit dynamic behaviors. The T3SS and specific effectors are important in shaping these behaviors early in the interaction when moderate relative humidity (60%–80%) is used. Spray-inoculated *Psy*B728a reside on leaf surfaces for 48 h prior to increasing in population size. From 24 to 48 h, a subset of bacteria expresses effectors. During this time period, a functional T3SS is required for a significant portion of the epiphytic population to survive, and HopAA1 and HopZ3 prevent an increase in the epiphytic population on *N. benthamiana*. In contrast, HopAA1 and HopZ3 are required for epiphytic survival on the nonhost tomato. Up to 72 h, endophytic colonization of *N. benthamiana* is rare and the population sizes of epiphytic and endophytic bacteria are not correlated. Furthermore, from 48 to 72 h, epiphytic *Psy*B728a populations can increase independently of whether bacteria significantly colonize the mesophyll region. Our data imply that there is an early and intimate interaction between bacteria and plant epidermal cells, in which the T3SS and effectors play an active role in affecting survival and/or growth in the epiphytic niche, prior to significant endophytic colonization.

Growth conditions play a critical role in the early population dynamics of *Psy*B728a after spray inoculation of plants. In contrast to our conditions, inoculation under high relative humidity conditions (>80%–100%) promotes immediate epiphytic growth of *Psy*B728a on snap bean leaf surfaces without a lag period (Beattie and Lindow, 1994). When snap bean plants are kept at high humidity until 48 h, *Psy*B728a not only grows rapidly to large populations on leaf surfaces within 48 h, but bacteria also invade the mesophyll region within 24 h after spray inoculation (Quiñones et al., 2004). In high humidity, bacteria might easily enter into the host plant's mesophyll region through stomata, rapidly multiply, and become released onto leaf surfaces.

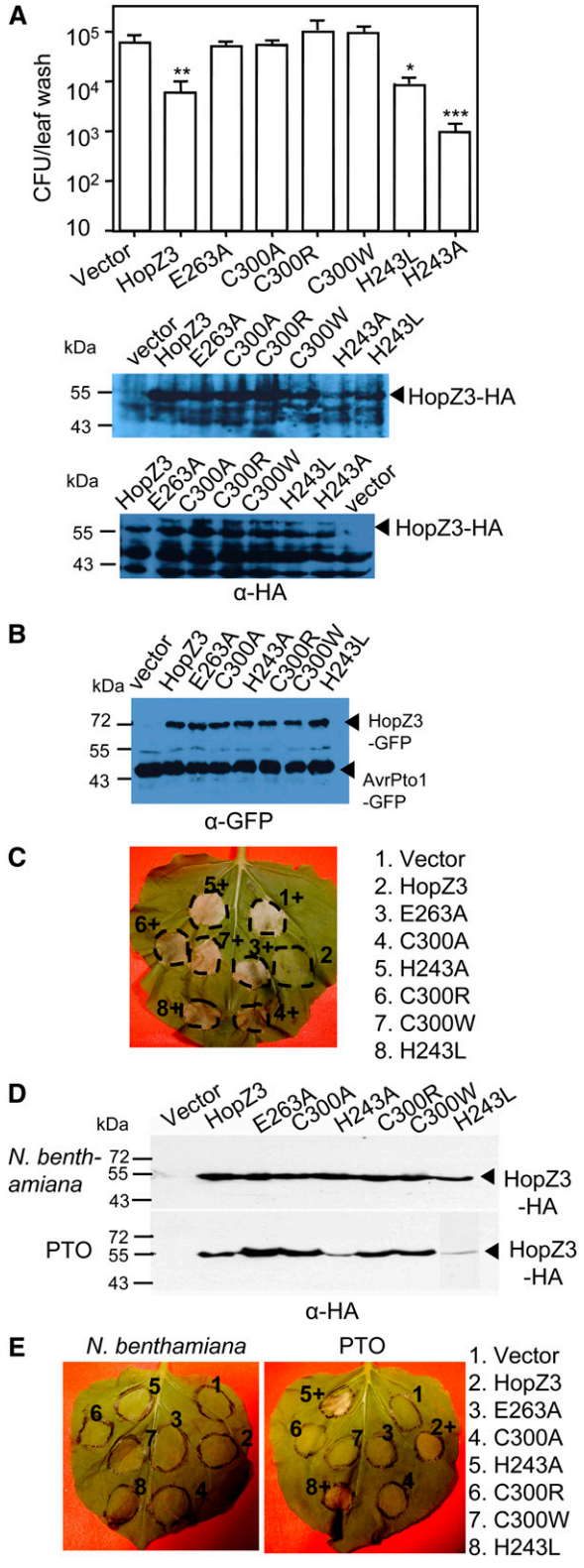

Figure 9. Conserved potential catalytic residues of HopZ3 are important for the function of HopZ3. A, Cys 300 and Glu 263 were important for HopZ3's effect on epiphytic bacteria growth. HopZ3$^-$ complemented with HopZ3-HA and HA-epitope-tagged point mutants driven by the constitutive npt2 promoter were sprayed onto *N. benthamiana* at an OD_{600} of 0.01. After 3 d, bacteria were quantified using leaf wash assays. An asterisk indicates significant differences from HopZ3$^-$ + vector at a given level (*$P < 0.05$, **$P < 0.005$, ***$P < 0.0001$, Mann-Whitney test, $n = 12$). HopZ3-HA and its variants were expressed in *P. syringae* shown by immunoblot analysis. Top blot, bacteria were grown in minimal media to mimic the plant environment. Bottom blot, bacteria were grown in KB media, similar to the conditions before spray inoculation. B, Immunoblot of extracts of *N. benthamiana* expressing HopZ3 and its variants or vector control cotransformed with AvrPto1-GFP. C, The ability of HopZ3 to interfere with AvrPto1-elicited cell death on *N. benthamiana* requires C, H, and E catalytic sites. AvrPto1-GFP and HopZ3-GFP or HopZ3-GFP variants were coexpressed after *A. tumefaciens*-mediated transient transformation. Representative pictures of the resulting cell death (indicated by +) are shown. D, Immunoblot analysis of extracts of plants expressing HopZ3 and its variants. Note that in the bottom section, lane H243L was exposed about 10-times longer than the other samples. For sections B and D, equal amounts of protein were resolved on 12% SDS-PAGE gels. E, The ability of HopZ3-HA to elicit cell death on Pto-expressing *N. benthamiana* depends on E263 and C300. Representative pictures showing the effect of HopZ3-HA and its variants on *N. benthamiana* with and without the tomato R-gene *Pto*. Cell death is indicated by +. These experiments were repeated at least three times with similar results.

Epiphytic communities play an important role in the transmission of pathogens, especially *P. syringae*, which can be carried in water droplets and may be part of the water cycle (Morris et al., 2008). More than 25 years ago, epiphytic bacterial populations of *P. syringae* were shown to be influenced by plant genotype in field studies (Daub and Hagedorn, 1981; Stadt and Saettler, 1981). Our study agrees with these results: *Psy*B728a shows larger epiphytic aggregates on *N. benthamiana* than are found on tomato. Furthermore, stimulating plant defenses using an SA agonist also restricts epiphytic fitness. Interestingly, epiphytic populations of *Xanthamonas axonopodis* on pepper (*Capsicum annuum*) are reduced in the field when specific effectors are deleted (Wichmann and Bergelson, 2004). However, because there is exchange between the epiphytic and endophytic populations as infections proceed, it was not clear from previous studies how and when the T3SS and specific effectors might influence bacterial populations in these two niches. Our work implicates a functional T3SS as important for early adaptation to and survival on leaf surfaces. We found no evidence that HopZ3 or HopAA1 affect bacterial release from the endophytic to the epiphytic pool. Since *Psy*B728a has numerous other effectors (Feil et al., 2005), one or more of these may have this role, similar to the effect of the AvrRpt2 effector, which promotes endophytic growth and release of *P. syringae* to susceptible Arabidopsis leaf surfaces (Guttman and Greenberg, 2001).

Direct imaging of GFP-labeled bacteria revealed the importance of the T3SS and specific effectors for the development of aggregates on leaf surfaces. On *N. benthamiana*, the very large aggregates of HopAA1$^-$ and HopZ3$^-$ strains and to some extent wild-type *Psy*B728a

Table II. *Cell death phenotype of HopZ3 and point mutants on N. benthamiana with and without Pto*

Protein Expressed	*N. benthamiana*[a]	*N. benthamiana/PTO*[a]
Vector	0/12	0/12
HopZ3	0/12	10/12 (mild cell death)
E263A	0/12	0/12
C300A	0/12	0/12
H243A	0/12	12/12 (strong cell death)
C300R	0/12	0/12
C300W	0/12	0/12
H243L	0/12	12/12 (strong cell death)

[a]Incidence of cell death out of the number of leaves tested.

resemble microbial biofilms observed in aquatic environments (Morris et al., 1998). Biofilms are communities of microorganisms with an exopolysaccharide matrix that protects the constituent bacteria from environmental stress, antibiotics, and host defenses (Parsek and Fuqua, 2004; Branda et al., 2005). More work is necessary to determine whether the very-large aggregates documented here are potentially developing into biofilms. However, on *N. benthamiana*, *Psy*B728a has more single cells (not in aggregates) than HopAA1$^-$ and HopZ3$^-$ strains. SA and components of innate immunity from animals can prevent bacterial biofilm development of *Pseudomonas aeruginosa* on glass coverslips and Arabidopsis roots (Singh et al., 2002; Prithiviraj et al., 2005). Similarly, epiphytic *Psy*B728a aggregates, possibly biofilms, might be affected by plant defenses that are induced by HopZ3 and/or HopAA1.

The growth dynamics and effector expression seen with *Psy*B728a may only be germane/relevant to some strains of *Pseudomonas* spp., mainly those with a strong epiphytic growth phase. Like *Psy*B728a, a subset of epiphytic *P. syringae* pv *phaseolicola* strain NP3121/*PavrPto-gfp* cells express GFP at 24 and 48 h, prior to endophytic colonization of *N. benthamiana* (J. Lee and J.T. Greenberg, unpublished data). Epiphytic expression of GFP in *Pph*NP3121/*PavrPto-gfp* was not previously observed when expression was examined 6 h after inoculation (Xiao et al., 2004). *P. syringae* pv *tomato* DC3000, a strain without a strong epiphytic phase (Roine et al., 1998; Boureau et al., 2002), shows a different effector expression pattern and colonization strategy. Epiphytic GFP expression from *Pto*DC3000 carrying *hrpA-gfp* (hrpA is a type-III-secreted protein that forms the secretion pilus; Lee et al., 2005) only occurs late in the infection, coincident with endophytic growth and highly developed disease lesions (Boureau et al., 2002). Because *Pto*DC3000 uses coronatine to gain rapid access to subepidermal regions (Melotto et al., 2006), this strain may not have the need to establish large epiphytic populations.

How might HopZ3 and HopAA1 function in plant cells to affect bacterial survival and growth? These effectors promote survival and possibly growth on tomato, a nonhost plant. This may be due to the presence of virulence targets of these effectors in tomato. However, any virulence activity of HopZ3 or HopAA1 is not enough to allow *Psy*B728a to cause significant disease on this host. HopZ3, which has sequence similarity to the YopJ Cys protease effector family, localizes to the nucleus and cell periphery, probably in the cytoplasm. However, dual subcellular localization might result from the high expression level used in this study. At least two other members of this effector family, PopP2 from *Ralstonia solanacaerum* and XopD from *Xanthomonas campestris* pv *vesicatoria* also localize to plant nuclei (Deslandes et al., 2003; Hotson et al., 2003). XopD possesses Small Ubiquitin-like Modifier (SUMO) isopeptidase activity (Hotson et al., 2003). PopP2 has acetyltransferase activity (Tasset et al., 2010). We were unable to detect significant Cys protease or SUMO protease activity of HopZ3, but we did detect acetyltransferase activity in vitro (J. Lee and J.T. Greenberg, unpublished data). Mutation of two residues that align with the conserved active site, E263 and C300, results in the loss of three phenotypes conferred by HopZ3. Thus, HopZ3 may have enzymatic activity on an as-yet-unknown substrate(s) or may require plant cofactors. Additionally, a third conserved residue, H243, is only required for suppressing cell death elicited by AvrPto1. YopJ has both SUMO protease and acetyltransferase activities (Mukherjee et al., 2006). It is possible that HopZ3 has more than one biochemical activity and that H243 is only essential for one of these activities.

HopAA1 lacks sequence similarity to proteins with any reported biochemical activity. Although HopAA1 from *Pto*DC3000 localizes to mitochondria when expressed in yeast (*Saccharomyces cerevisiae*; Munkvold et al., 2008), there was no evidence for such localization in plants. In contrast, like some effectors that modulate host signaling (Maurer-Stroh and Eisenhaber, 2004), HopAA1 localizes to the plant cell periphery, probably the plasma membrane. HopAA1 and its orthologs are predicted to have one to three conserved membrane-spanning regions and at least one extracellular region. Interestingly, the *Escherichia coli* TIR effector localizes to the host plasma membrane and forms a receptor with a predicted extracellular loop region for *E. coli* to dock (Kenny et al., 1997). Whether HopAA1 has a similar specialized function due to its possible architectural similarity to TIR1 awaits further investigation.

In summary, the T3SS and individual effectors are important for *Psy*B728a bacteria to survive and grow on leaf surfaces. This raises the question as to how the T3SS functions across the plant cuticle. Several different bacterial epiphytes can alter leaf surface properties and affect cuticle permeability (Schreiber et al., 2005). We hypothesize that *Psy*728a can also modify cuticle properties to allow access of the T3SS secretion needle to the plant epidermal cell membrane. Alteration of the cuticle is consistent with the induction of the effector reporter expressed in epiphytic *Psy*B728a, since infection of Arabidopsis with reduced cutin, a cuticle component, results in strong induction of this

reporter in another *P. syringae* strain (Xiao et al., 2004). Further characterization of how *Psy*B728a adapts to and alters leaf surfaces will be informative to understanding early events in the infection process.

MATERIALS AND METHODS

Bacterial Strains and Growth Conditions

The bacterial strain *Psy*B728a and its previously characterized derivatives deleted for HopAA1 or HopZ3 or harboring an insertion in T3SS component HrcC (Hirano et al., 1999; Vinatzer et al., 2006) were grown on solid agar and liquid King's broth (KB; King et al., 1954) with 34 μg/mL rifampicin at 30°C. *Pseudomonas syringae* strains were tagged with GFP using the *Ptrp-gfp* plasmid (to achieve constitutive GFP; Miller et al., 2000) or the *PavrPto-gfp* plasmid (to monitor effector gene expression; Xiao et al., 2004) by electroporation using 2.5 kV, 500 , and 10 μF. GFP-tagged strains were grown using 50 μg/mL kanamycin.

Agrobacterium tumefaciens C58C1 was used to express HopZ3 and its derivatives, HopAA1, AvrPto1, and/or Pto transiently in plants. *A. tumefaciens* was grown in Luria-Bertani broth (Sambrook et al., 1989) with 50 μg/mL kanamycin at 30°C.

Plant Genotypes and Growth Conditions

Nicotiana benthamiana and tomato (*Solanum lycopersicom* '76R') were grown in a walk-in growth chamber kept at 24°C, 60% to 80% relative humidity, and with 16-h day light. Plants were grown for 3 weeks for *P. syringae* infection assays and for 4 weeks for expression of proteins with *A. tumefaciens*-mediated transient transformation.

Transgenic *N. benthamiana* containing the tomato *R* gene *Pto* was developed using a similar method to that described previously (Thilmony et al., 1995).

Epiphytic Bacteria Population Assays

Overnight cultures of GFP-tagged *Psy*B728a and its derivatives were diluted 1:10 and grown for 2 h at 30°C. To make the inocula, cells were collected by centrifugation and resuspended in 10 mM $MgSO_4$ to an optical density at 600 nm (OD_{600}) of 0.01. Inocula were sprayed with spray bottles onto the tops of the first through fourth leaves of *N. benthamiana* plants (17–21 d old). Plants were sprayed to run-off to completely soak the leaves (about 1 mL per plant), covered with a dome with holes, and maintained at a relative humidity of 60% to 80%.

Epiphytic bacteria were quantified from leaf discs from independent plants using leaf wash (8-mm diameter discs, n = 10–12) and/or microscopy assays (12-mm diameter discs, n = 6–8 with at least three random images per disc analyzed). For the wash assay, each leaf disc was placed into 1 mL 10 mM $MgSO_4$ and vortexed for 5 s at maximum speed to remove the attached biomass. Samples were serially diluted and enumerated by viable counts after plating on KB agar. Sonication was also evaluated as a method for harvesting epiphytic bacteria, but this approach was less effective than vortexing for harvesting aggregates >10 μm^2. For the microscopy assay, each leaf disc placed onto a microscope slide adaxial side up was covered with 1% agar and a coverslip was placed on the top (Monier and Lindow, 2003). Samples were then viewed with a Zeiss Axioskop epifluorescence microscope (Carl Zeiss) or Zeiss 510 laser-scanning confocal microscope using 400× or 630× magnification, respectively. For the epifluorescence microscopy, GFP was visualized using a 450 to 490 nm excitation, 515 nm emission filter (fluorescein isothiocyanate filter set). Images were captured with an AxioCAM HRC video camera (Zeiss) and data were processed with Axio vision Rel.4.6 software. For the confocal microscopy, GFP fluorescence was visualized by excitation using a single line 488-nm laser, and emission was collected with filter set to a 505 to 550 nm bandpass. The chlorophyll autofluorescence was excited with a single line 543 laser, and emission were collected at wavelengths >615 nm. Horizontal (x-y) images were taken at 0.5-μm intervals. Vertical cross-section (x-z) images were generated with a laser scanning microscope image browser.

Dead epiphytic bacteria were stained by placing leaf discs adaxial side down in 200 μL of 330 μg/mL propidium iodide (Invitrogen) in phosphate-buffered saline (PBS) for 15 min in the dark and washing once in 200 μL PBS prior to embedding in 1% agar. Stained bacteria were visualized by epifluorescence microscopy using excitation at 515 to 560 nm and emission at 590 nm (Rhodamine filter set).

To perform quantitative analysis of GFP-tagged bacteria, random micrographs along transect of the leaves were taken as representative images of the attached bacterial populations. The area of green fluorescence was used to quantify the amount bacteria present on leaf surfaces. While there was some green autofluorescence from the leaves, this was diffuse and not as bright as the bacteria. The autofluorescence dropped out of the green-fluorescing area during image analysis because it was below the threshold value used.

Analysis of Micrographs

Bacterial area was quantified from epifluorescence micrographs using ImageJ available online from the National Institutes of Health. Images were thresholded using a maximum entropy threshold function developed by Jerek Sacha that is available on the ImageJ Web site. The area of the pixels that fluoresced green above the threshold amount were quantified using the analyze particles function. An example of an image used in the analysis is shown in Supplemental Figure S12.

BTH Treatment of Plants

N. benthamiana that was 17 to 21 d old was sprayed with 100 μM BTH (a kind gift from Robert Dietrich, Syngenta, Research Triangle Park, NC) dissolved in water. After 24 h, plants were sprayed with *Psy*B728a and sampled as described above.

Release of Endophytic Bacteria onto Leaf Surfaces

Leaves of 4-week-old *N. benthamiana* were sterilized by spraying with 70% ethanol and then infiltrated with *Psy*B728a and its derivatives at an OD_{600} of 0.00001 using a needleless syringe. The leaves were wiped with 70% ethanol again to remove any surface bacteria and examined to ensure that GFP-marked bacteria were absent from the surface. Release of bacteria to leaf surfaces was monitored by leaf washes and epifluorescence microscopy (see above).

Attachment Assays

The ability of *Psy*B728a and its derivatives to attach to surfaces was assayed by examining attachment to glass and plastic substrates. For the plastic surface, 400 μL of an 0.1 OD_{600} culture in minimal media (Mudgett and Staskawicz, 1999) was added to wells of a 48-well tissue culture plate (Corning Life Sciences). Plates were incubated for 24 h at 20°C with shaking. The supernatant was removed and the attached biomass was washed three times with PBS. Attached biomass was then stained with 1% crystal violet for 20 min at room temperature and then washed another three times with PBS. The crystal violet was resuspended by dissolving it in 95% ethanol for 2 min at room temperature with shaking and then quantified by measuring the A_{600}.

For the glass surface assay, *P. syringae* strains were grown overnight in minimal media (Mudgett and Staskawicz, 1999) at 20°C. The coverslips were immersed in 1 mL of 0.1 OD_{600} culture cell and allowed to attach to the coverslips for 3 h at 20°C. Then the coverslips were washed three times in minimal media to remove unattached bacteria. The coverslips were then transferred to microscope slides and viewed with epifluorescence microscopy.

Construction of Point Mutants in HopZ3

Single amino acid changes in the catalytic domains of HopZ3 were made using the Stratagene quick change kit. Point mutants were created from HopZ3 that was cloned into the pDONR207 Gateway donor vector (Invitrogen; Vinatzer et al., 2006).Cys 300 was changed to Trp (C300W) using the forward primer CAATACTCGAAAACTGACTGGACCATGTTTGCGC and reverse primer GCGCAAACATGGTCCAGTCAGTTTTCGAGTATTG, both 5′ to 3′. The catalytic His at 243AA was changed to Leu (H243L) using the forward primer CAAAAAGATGCCAGACCTCCATATAGCCTTGGATATC and reverse primer GATATCCAAGGCTATATGGAGGTCTGGCATCTTTTTG, both 5′ to 3′. Glu 263 was changed to Ala (E263A) using the forward primer GATTGTCGGCTTT GCGTCTGCCCCTGGGAAC and reverse primer GTTCCCAGGGGCAGACGC AAAGCCGACAATC, both 5′ to 3′. Point mutants were constructed using the specification in the manufacturer's manual and using 16 cycles of amplification.

In addition, point mutations were also made in HopZ3 in pDONR207 using the GeneTailor kit (Invitrogen). Cys 300 was changed to Ala (C300A) using the forward primer TCAATACTCGAAAACTGACGCCACCATGTTTGC and the reverse primer GTCAGTTTTCGAGTATTGAAGAAAATTTCCTACC, both 5′ to 3′. His 243 was changed to Ala (H243A) using the forward primer TTCAAAAAGATGCCAGACGCCCATATAGCCTTG and the reverse primer GTCTGGCATCTTTTTGAATGGGGGGTAAAC. HopZ3 point mutants were sequence validated and transferred into Gateway vectors (pBAV154, pBAV150, and pBAV226) for expression in *A. tumefaciens* and *P. syringae* following the method described in the Gateway manual (Invitrogen). HopZ3 point mutants were transferred into two vectors for expression in *A. tumefaciens*, pBAV154 and pBAV150. pBAV154 is a dexamethasone-inducible vector with a C-terminal HA tag, while pBAV150 is a dexamethasone-inducible vector with a C-terminal GFP tag (Vinatzer et al., 2006). Electroporation of plasmids into *A. tumefaciens* C58C1 was achieved using 2.5 kV, 400 , and 25 μF. For expression in *P. syringae*, HopZ3 point mutants were transferred into pBAV226, a low-copy-number expression vector that has an *npt*II promoter (Vinatzer et al., 2006) and a C-terminal HA tag. Plasmids were electroporated into *Psy*B728a as described above.

Transient Expression Assays, Western Analysis, and Membrane Fractionation

A. tumefaciens C58C1 containing effectors in pBAV154 or pBAV150 was grown in liquid culture in Luria-Bertani broth with kanamycin overnight at 30°C. One milliliter of overnight culture was added to 3 mL induction medium (Vinatzer et al., 2006) containing 50 μg/mL acetosyringone and placed at 30°C to induce for 5 h. An infiltration inoculum was made by collecting induced cells by centrifugation and resuspending them in infiltration medium (Vinatzer et al., 2006) at an OD_{600} of 0.4. Inocula were infiltrated into 4-week-old *N. benthamiana* with a needleless syringe. For HopAA1 expression, samples for immunoblot analysis were taken at 24 h and cell death was scored visually after 48 h. For all other experiments involving cell death, plants were treated with 30 μM dexamethasone and 0.1% Tween 20 in water (dex) 2 d after *A. tumefaciens* infiltration. Cell death was scored by visual inspection on d 4 after dex treatments. For immunoblots, samples were taken 12 h after dex treatments.

For immunoblot studies, two 8-mm leaf disks were ground to a uniform consistency in 50 μL of resuspension buffer (Vinatzer et al., 2006). Cellular debris was removed by centrifugation, and supernatant was mixed with SDS sample buffer (Lewis et al., 2008). Equal amounts of extract for each sample were separated by eletrophoresis and were transferred to a polyvinylidene fluoride membrane (Millipore Corporation). Membranes were probed with a primary, anti-HA monoclonal antibody (Covance) at a dilution of 1:5,000, followed by a secondary, anti-mouse HRP (Pierce) at a 1:5,000 dilution.

Membrane fractionation was performed as described (Lewis et al., 2008). GFP monoclonal antibody (Covance) was used at a 1:5,000 dilution and secondary anti-rabbit antibody (Pierce) at a 1:5,000 dilution. Visualization of immunoreaction was achieved by ECL (Pierce).

For microscopy analysis, nuclei were counterstained with 10 μg/mL Hoechst 33342 solution in water (Invitrogen). Fluorescence was analyzed with UV (365-nm excitation, 420-nm emission) or fluorescein isothiocyanate filter sets.

Yeast Interaction Tests

Possible interactions between Pto and HopZ3 or AvrB3 were tested using yeast (*Saccharomyces cerevisiae*) two-hybrid assays using the LEXA system as described (Xiao et al., 2007).

Detection of *Pto* Expression

Total RNA from plant tissues was extracted using TRIzol (Invitrogen) reagent. RNA was converted into cDNA with Thermoscript reverse transcriptase (Invitrogen), and reverse transcription-PCR was performed to amplify the Pto transcripts with 25 PCR cycles using the Pto-specific primers (5′-GAATATCCAAGAAAGGGACT-3′ and 5′-TGGAGACGAAGTGCATACTC-3′). Actin (5′-TGGACTCTGGTGATGGTGTC-3 and CCTCCAATCCAAACACTGTA-3′) was amplified as a control.

Author-Recommended Internet Resources

The authors recommend the following Web sites: National Institutes of Health ImageJ Web site, http://rsbweb.nih.gov/ij/; Web site for maximum entropy threshold, http://rsbweb.nih.gov/ij/plugins/entropy.html; transmembrane prediction, http://www.ch.embnet.org/software/TMPRED_form.html; and topology prediction of membrane proteins, http://mobyle.pasteur.fr/cgi-bin/MobylePortal/portal.py?form=toppred.

Sequence data from this article can be found in the GenBank/EMBL data libraries under accession numbers HopZ3 (GI:66044472), HopAA1 (GI:66044434), AvrPto1 (GI:66048143), AvrB3 GI:79093592, and PTO (GI:8547226).

Supplemental Data

The following materials are available in the online version of this article.

Supplemental Figure S1. Examples of GFP-labeled microcolonies associated with substomatal chambers or mesophyll cells and bacteria being released from the endophytic pool to leaf surfaces.

Supplemental Figure S2. Comparison of bacterial populations of *Psy*B728a carrying *Ptrp-gfp* and *PavrPto-gfp* inoculated on *N. benthamiana* leaf surface.

Supplemental Figure S3. Lack of evidence for epidermal cell death at 48 h after spray inoculation with *Psy*B728a.

Supplemental Figure S4. Examples of the association of GFP-expressing bacteria with different epidermal cell types.

Supplemental Figure S5. Enumeration of epiphytic and endophytic bacterial populations after spray inoculation show that epiphytic but not endophytic bacterial populations of HopAA1$^-$, HopZ3$^-$, and HrcC$^-$ are different from *Psy*B728a at 48 h.

Supplemental Figure S6. Fluorescence micrographs showing the effects of HopAA1$^-$, HopZ3$^-$, and HrcC$^-$ mutations on the release of endophytic bacteria onto *N. benthamiana* leaf surfaces.

Supplemental Figure S7. Confocal section of a HopAA1-GFP-expressing *N. benthamiana* epidermal cell.

Supplemental Figure S8. Localization of variants of HopZ3-GFP expressed in *N. benthamiana*.

Supplemental Figure S9. Validation that *Pto* is expressed in transgenic *N. benthamiana* harboring *Pto*.

Supplemental Figure S10. Cell death elicitation by AvrB3 on Pto-expressing *N. benthamiana*.

Supplemental Figure S11. Lack of interaction of Pto with AvrB3 or HopZ3 in yeast.

Supplemental Figure S12. Example of image processing to visualize GFP-tagged bacteria.

Supplemental Table S1. Cell death phenotype elicited by HopZ3 (or HopZ3 variants) and Pto after coexpression on *N. benthamiana*.

ACKNOWLEDGMENTS

We thank Dr. Steve Lindow (University of California, Berkeley) for useful discussions, reagents, and advice on imaging epiphytic bacteria. We thank Drs. Jian-Min Zhou (National Institute of Biological Science, Beijing, China) and Xiaoyan Tang (Kansas State University) for providing *PavrPto-gfp*; Drs. Joanna Jelenska, Ho Won Jung, and Boris A. Vinatzer (Virginia Tech) for helpful comments on the manuscript; and Ru Yi Teow and Vytas Bindokas (Integrated Microscopy Core Facility at the University of Chicago) for help with the confocal microscopy.

Received November 3, 2011; accepted February 7, 2012; published February 7, 2012.

LITERATURE CITED

Abramovitch RB, Anderson JC, Martin GB (2006) Bacterial elicitation and evasion of plant innate immunity. Nat Rev Mol Cell Biol **7:** 601–611

Beattie GA, Lindow SE (1994) Survival, growth and localization of epiphytic

fitness mutants of Pseudomonas syringae on leaves. Appl Environ Microbiol **60:** 3790–3798

Boureau T, Routtu J, Roine E, Taira S, Romantschuk M (2002) Localization of hrpA-induced *Pseudomonas syringae* pv. *tomato* DC3000 in infected tomato leaves. Mol Plant Pathol **3:** 451–460

Branda SS, Vik S, Friedman L, Kolter R (2005) Biofilms: the matrix revisited. Trends Microbiol **13:** 20–26

Caplan J, Padmanabhan M, Dinesh-Kumar SP (2008) Plant NB-LRR immune receptors: from recognition to transcriptional reprogramming. Cell Host Microbe **3:** 126–135

Chang WS, van de Mortel M, Nielsen L, Nino de Guzman G, Li X, Halverson LJ (2007) Alginate production by *Pseudomonas putida* creates a hydrated microenvironment and contributes to biofilm architecture and stress tolerance under water-limiting conditions. J Bacteriol **189:** 8290–8299

Chen Z, Kloek AP, Boch J, Katagiri F, Kunkel BN (2000) The *Pseudomonas syringae* avrRpt2 gene product promotes pathogen virulence from inside plant cells. Mol Plant Microbe Interact **13:** 1312–1321

Chisholm ST, Coaker G, Day B, Staskawicz BJ (2006) Host-microbe interactions: shaping the evolution of the plant immune response. Cell **124:** 803–814

Daub M, Hagedorn D (1981) Epiphytic population of *Pseudomonas syringae* on susceptible and resistant bean lines. Phytopathology **71:** 547–550

Delaney TP, Uknes S, Vernooij B, Friedrich L, Weymann K, Negrotto D, Gaffney T, Gut-Rella M, Kessmann H, Ward E, et al (1994) A central role of salicylic acid in plant disease resistance. Science **266:** 1247–1250

Deslandes L, Olivier J, Peeters N, Feng DX, Khounlotham M, Boucher C, Somssich I, Genin S, Marco Y (2003) Physical interaction between RRS1-R, a protein conferring resistance to bacterial wilt, and PopP2, a type III effector targeted to the plant nucleus. Proc Natl Acad Sci USA **100:** 8024–8029

Dulla G, Lindow SE (2008) Quorum size of *Pseudomonas syringae* is small and dictated by water availability on the leaf surface. Proc Natl Acad Sci USA **105:** 3082–3087

Feil H, Feil WS, Chain P, Larimer F, DiBartolo G, Copeland A, Lykidis A, Trong S, Nolan M, Goltsman E, et al (2005) Comparison of the complete genome sequences of *Pseudomonas syringae* pv. *syringae* B728a and pv. *tomato* DC3000. Proc Natl Acad Sci USA **102:** 11064–11069

Feys BJ, Moisan LJ, Newman MA, Parker JE (2001) Direct interaction between the Arabidopsis disease resistance signaling proteins, EDS1 and PAD4. EMBO J **20:** 5400–5411

Friedrich L, Lawton K, Wilhelm R, Masner P, Specker N, Gut Rella M, Meier B, Dincher S, Staub T, Uknes S, et al (1996) A benzothiadiazole derivative induces systemic acquired resistance. Plant J **10:** 61–70

Greenberg JT, Vinatzer BA (2003) Identifying type III effectors of plant pathogens and analyzing their interaction with plant cells. Curr Opin Microbiol **6:** 20–28

Greenberg JT, Yao N (2004) The role and regulation of programmed cell death in plant-pathogen interactions. Cell Microbiol **6:** 201–211

Guttman DS, Greenberg JT (2001) Functional analysis of the type III effectors AvrRpt2 and AvrRpm1 of *Pseudomonas syringae* with the use of a single-copy genomic integration system. Mol Plant Microbe Interact **14:** 145–155

He SY, Huang HC, Collmer A (1993) *Pseudomonas syringae* pv. *syringae* harpinPss: a protein that is secreted via the Hrp pathway and elicits the hypersensitive response in plants. Cell **73:** 1255–1266

Hirano SS, Charkowski AO, Collmer A, Willis DK, Upper CD (1999) Role of the Hrp type III protein secretion system in growth of *Pseudomonas syringae* pv. *syringae* B728a on host plants in the field. Proc Natl Acad Sci USA **96:** 9851–9856

Hotson A, Chosed R, Shu H, Orth K, Mudgett MB (2003) Xanthomonas type III effector XopD targets SUMO-conjugated proteins in planta. Mol Microbiol **50:** 377–389

Kenny B, DeVinney R, Stein M, Reinscheid DJ, Frey EA, Finlay BB (1997) *Enteropathogenic* E. coli (EPEC) transfers its receptor for intimate adherence into mammalian cells. Cell **91:** 511–520

King EO, Ward MK, Raney DE (1954) Two simple media for the demonstration of phyocyanin and fluorescin. J Lab Clin Med **44:** 201–207

Lawton KA, Friedrich L, Hunt M, Weymann K, Delaney T, Kessmann H, Staub T, Ryals J (1996) Benzothiadiazole induces disease resistance in Arabidopsis by activation of the systemic acquired resistance signal transduction pathway. Plant J **10:** 71–82

Lee J, Klusener B, Tsiamis G, Stevens C, Neyt C, Tampakaki AP, Panopoulos NJ, Nöller J, Weiler EW, Cornelis GR, et al (2001) HrpZ (Psph) from the plant pathogen *Pseudomonas syringae* pv. *phaseolicola* binds to lipid bilayers and forms an ion-conducting pore in vitro. Proc Natl Acad Sci USA **98:** 289–294

Lee MW, Jelenska J, Greenberg JT (2008) Arabidopsis proteins important for modulating defense responses to *Pseudomonas syringae* that secrete HopW1-1. Plant J **54:** 452–465

Lee YH, Kolade OO, Nomura K, Arvidson DN, He SY (2005) Use of dominant-negative HrpA mutants to dissect Hrp pilus assembly and type III secretion in *Pseudomonas syringae* pv. *tomato*. J Biol Chem **280:** 21409–21417

Lewis JD, Abada W, Ma W, Guttman DS, Desveaux D (2008) The HopZ family of *Pseudomonas syringae* type III effectors require myristoylation for virulence and avirulence functions in *Arabidopsis thaliana*. J Bacteriol **190:** 2880–2891

Lin NC, Martin GB (2007) Pto- and Prf-mediated recognition of AvrPto and AvrPtoB restricts the ability of diverse *pseudomonas syringae* pathovars to infect tomato. Mol Plant Microbe Interact **20:** 806–815

Maurer-Stroh S, Eisenhaber F (2004) Myristoylation of viral and bacterial proteins. Trends Microbiol **12:** 178–185

Melotto M, Underwood W, Koczan J, Nomura K, He SY (2006) Plant stomata function in innate immunity against bacterial invasion. Cell **126:** 969–980

Miller WG, Leveau JH, Lindow SE (2000) Improved gfp and inaZ broad-host-range promoter-probe vectors. Mol Plant Microbe Interact **13:** 1243–1250

Monier JM, Lindow SE (2003) Differential survival of solitary and aggregated bacterial cells promotes aggregate formation on leaf surfaces. Proc Natl Acad Sci USA **100:** 15977–15982

Monier JM, Lindow SE (2004) Frequency, size, and localization of bacterial aggregates on bean leaf surfaces. Appl Environ Microbiol **70:** 346–355

Morris CE, Monier JM (2003) The ecological significance of biofilm formation by plant-associated bacteria. Annu Rev Phytopathol **41:** 429–453

Morris CE, Monier JM, Jacques MA (1998) A technique to quantify the population size and composition of the biofilm component in communities of bacteria in the phyllosphere. Appl Environ Microbiol **64:** 4789–4795

Morris CE, Sands DC, Vinatzer BA, Glaux C, Guilbaud C, Buffière A, Yan S, Dominguez H, Thompson BM (2008) The life history of the plant pathogen *Pseudomonas syringae* is linked to the water cycle. ISME J **2:** 321–334

Mudgett MB, Staskawicz BJ (1999) Characterization of the *Pseudomonas syringae* pv. *tomato* AvrRpt2 protein: demonstration of secretion and processing during bacterial pathogenesis. Mol Microbiol **32:** 927–941

Mukherjee S, Keitany G, Li Y, Wang Y, Ball HL, Goldsmith EJ, Orth K (2006) *Yersinia* YopJ acetylates and inhibits kinase activation by blocking phosphorylation. Science **312:** 1211–1214

Munkvold KR, Martin ME, Bronstein PA, Collmer A (2008) A survey of the *Pseudomonas syringae* pv. *tomato* DC3000 type III secretion system effector repertoire reveals several effectors that are deleterious when expressed in *Saccharomyces cerevisiae*. Mol Plant Microbe Interact **21:** 490–502

Nawrath C, Métraux JP (1999) Salicylic acid induction-deficient mutants of *Arabidopsis* express PR-2 and PR-5 and accumulate high levels of camalexin after pathogen inoculation. Plant Cell **11:** 1393–1404

Nomura K, Melotto M, He SY (2005) Suppression of host defense in compatible plant-*Pseudomonas syringae* interactions. Curr Opin Plant Biol **8:** 361–368

Parsek MR, Fuqua C (2004) Biofilms 2003: emerging themes and challenges in studies of surface-associated microbial life. J Bacteriol **186:** 4427–4440

Prithiviraj B, Bais HP, Weir T, Suresh B, Najarro EH, Dayakar BV, Schweizer HP, Vivanco JM (2005) Down regulation of virulence factors of *Pseudomonas aeruginosa* by salicylic acid attenuates its virulence on *Arabidopsis thaliana* and *Caenorhabditis elegans*. Infect Immun **73:** 5319–5328

Quiñones B, Pujol CJ, Lindow SE (2004) Regulation of AHL production and its contribution to epiphytic fitness in Pseudomonas syringae. Mol Plant Microbe Interact **17:** 521–531

Rate DN, Greenberg JT (2001) The *Arabidopsis aberrant growth and death2* mutant shows resistance to *Pseudomonas syringae* and reveals a role for NPR1 in suppressing hypersensitive cell death. Plant J **27:** 203–211

Roine E, Raineri DM, Romantschuk M, Wilson M, Nunn DN (1998) Characterization of type IV pilus genes in *Pseudomonas syringae* pv. *tomato* DC3000. Mol Plant Microbe Interact **11:** 1048–1056

Rosebrock TR, Zeng L, Brady JJ, Abramovitch RB, Xiao F, Martin GB (2007) A bacterial E3 ubiquitin ligase targets a host protein kinase to disrupt plant immunity. Nature **448:** 370–374

Sambrook J, Fritsch EF, Maniatis T (1989) Molecular Cloning, a Laboratory Manual, Ed 2. Cold Spring Harbor Laboratory Press, Cold Spring Harbor, NY

Schellenberg B, Ramel C, Dudler R (2010) *Pseudomonas syringae* virulence factor syringolin A counteracts stomatal immunity by proteasome inhibition. Mol Plant Microbe Interact **23:** 1287–1293

Schreiber L, Krimm U, Knoll D, Sayed M, Auling G, Kroppenstedt RM (2005) Plant-microbe interactions: identification of epiphytic bacteria and their ability to alter leaf surface permeability. New Phytol **166:** 589–594

Singh PK, Parsek MR, Greenberg EP, Welsh MJ (2002) A component of innate immunity prevents bacterial biofilm development. Nature **417:** 552–555

Stadt S, Saettler A (1981) Effect of host genotype on multiplication of *Pseudomonas phaseolicola*. Phytopathology **71:** 1307–1310

Tang X, Xie M, Kim YJ, Zhou J, Klessig DF, Martin GB (1999) Overexpression of Pto activates defense responses and confers broad resistance. Plant Cell **11:** 15–29

Tasset C, Bernoux M, Jauneau A, Pouzet C, Brière C, Kieffer-Jacquinod S, Rivas S, Marco Y, Deslandes L (2010) Autoacetylation of the *Ralstonia solanacearum* effector PopP2 targets a lysine residue essential for RRS1-R-mediated immunity in *Arabidopsis*. PLoS Pathog **6:** e1001202

Thilmony RL, Chen Z, Bressan RA, Martin GB (1995) Expression of the tomato Pto gene in tobacco enhances resistance to *Pseudomonas syringae* pv *tabaci* expressing avrPto. Plant Cell **7:** 1529–1536

Uknes S, Mauch-Mani B, Moyer M, Potter S, Williams S, Dincher S, Chandler D, Slusarenko A, Ward E, Ryals J (1992) Acquired resistance in *Arabidopsis*. Plant Cell **4:** 645–656

Vinatzer BA, Teitzel GM, Lee MW, Jelenska J, Hotton S, Fairfax K, Jenrette J, Greenberg JT (2006) The type III effector repertoire of *Pseudomonas syringae* pv. *syringae* B728a and its role in survival and disease on host and non-host plants. Mol Microbiol **62:** 26–44

Wichmann G, Bergelson J (2004) Effector genes of *Xanthomonas axonopodis* pv. *vesicatoria* promote transmission and enhance other fitness traits in the field. Genetics **166:** 693–706

Wilson M, Hirano SS, Lindow SE (1999) Location and survival of leaf-associated bacteria in relation to pathogenicity and potential for growth within the leaf. Appl Environ Microbiol **65:** 1435–1443

Wright DJ, Smith SC, Joardar V, Scherer S, Jervis J, Warren A, Helm RF, Potts M (2005) UV irradiation and desiccation modulate the three-dimensional extracellular matrix of *Nostoc commune* (Cyanobacteria). J Biol Chem **280:** 40271–40281

Xiao F, Goodwin SM, Xiao Y, Sun Z, Baker D, Tang X, Jenks MA, Zhou JM (2004) Arabidopsis CYP86A2 represses *Pseudomonas syringae* type III genes and is required for cuticle development. EMBO J **23:** 2903–2913

Xiao F, He P, Abramovitch RB, Dawson JE, Nicholson LK, Sheen J, Martin GB (2007) The N-terminal region of *Pseudomonas* type III effector AvrPtoB elicits Pto-dependent immunity and has two distinct virulence determinants. Plant J **52:** 595–614

Yu J, Penaloza-Vazquez A, Chakrabarty AM, Bender CL (1999) Involvement of the exopolysaccharide alginate in the virulence and epiphytic fitness of *Pseudomonas*. Mol Microbiol **33:** 712–720